Biotechnology Frontiers
OPEN ACCESS
ISSN 3117-5791
Original Research Article
Check for updates

In Silico ADMET and Molecular Docking Studies of Thiazolidinone Derivatives as Potential Antitubercular Agents

Valarmathy Joshua*[1], L. Samuel Joshua[1], Sherlyn Joshua[2], and Vinolyn Joshua[2]

[1]*Medicinal Chemistry Research Laboratory, Department of Pharmaceutical Chemistry, Sri Venkateswaraa Faculty of Pharmacy, Ettayapuram – 628902, Tamil Nadu, India*
[2]*UV Gullas College of Medicine, 6014 Mandaue City, Cebu, Philippines*

Corresponding author: **Valarmathy Joshua** | E-mail: **valarmathyjoshua@gmail.com**

Citation: Valarmathy Joshua, L. Samuel Joshua, Sherlyn Joshua, and Vinolyn Joshua (2025). *In Silico* ADMET and Molecular Docking Studies of Thiazolidinone Derivatives as Potential Antitubercular Agents. *Biotechnology Frontiers: An International Journal.*
DOI: https://doi.org/10.51470/BF.2025.5.2.43

14 August 2025: Received | 19 September 2025: Revised | 17 October 2025: Accepted | 13 November 2025: Available Online

Abstract

Tuberculosis (TB) remains one of the leading infectious diseases worldwide, necessitating the continuous development of novel antitubercular agents with improved efficacy and safety profiles. In the present investigation, a series of novel N-(4-oxo-3-aryl-1,2-thiazolidin-2-yl) pyridine-3-carboxamide derivatives 3(a–e) were synthesized and evaluated for their antitubercular potential. The synthesized compounds were characterized by physicochemical parameters, FT-IR spectroscopy, and ^{1}H NMR spectral analysis, which confirmed the successful formation of the desired thiazolidinone derivatives. The synthesized compounds were screened for antitubercular activity against Mycobacterium tuberculosis H37Rv strain using the Resazurin Microtiter Assay (REMA) plate method. Among the tested derivatives, compounds 3a and 3d exhibited significant antitubercular activity, while compounds 3b and 3c demonstrated moderate to good activity and compound 3e showed moderate activity. In silico studies, including Molinspiration physicochemical evaluation, bioactivity prediction, ADMET analysis, and molecular docking studies, were carried out to assess the drug-likeness and pharmacokinetic properties of the synthesized molecules. Molecular docking studies were performed using AutoDock Vina software to evaluate ligand–protein interactions and binding affinity toward the selected target protein. All compounds obeyed Lipinski's Rule of Five with zero violations and showed favourable oral bioavailability parameters. ADMET predictions indicated high predicted intestinal absorption, acceptable distribution profiles, absence of predicted hERG inhibition indicating low cardiotoxicity risk, and non-mutagenic behaviour for most compounds. Molecular docking studies demonstrated favourable binding affinities toward the target protein, with docking scores ranging from –5.7 to –8.6 kcal/mol. Compounds 3a and 3b exhibited the best docking scores, while compounds 3a and 3d demonstrated significant in vitro antitubercular activity, indicating favourable ligand–protein interactions. The combined experimental and computational findings suggest that the synthesized thiazolidinone derivatives possess promising antitubercular potential and may serve as valuable lead molecules for further optimization and development of novel anti-TB agents.

Keywords: *Thiazolidinone derivatives; FT-IR spectroscopy; ^{1}H NMR spectroscopy; Antitubercular activity; REMA assay; Mycobacterium tuberculosis; Molecular docking; AutoDock Vina; ADMET prediction; Drug-likeness..*

1. Introduction

Tuberculosis (TB) is a chronic infectious disease caused primarily by *Mycobacterium tuberculosis*, which mainly affects the lungs but may also involve other organs of the body. According to the World Health Organization (WHO), tuberculosis remains one of the leading causes of death from infectious diseases worldwide, with millions of new cases reported annually. Despite the availability of several therapeutic agents, tuberculosis continues to be a major cause of morbidity and mortality, particularly in developing countries. The emergence of multidrug-resistant tuberculosis (MDR-TB) and extensively drug-resistant tuberculosis (XDR-TB) has become a major global health challenge, reducing the effectiveness of existing therapies and emphasizing the urgent need for the discovery of novel antitubercular agents with improved efficacy, reduced toxicity, and better pharmacokinetic properties [1-7]. Heterocyclic compounds play an essential role in medicinal chemistry because of their broad spectrum of biological activities. Among these, thiazolidinone derivatives have attracted considerable attention due to their diverse pharmacological properties, including antimicrobial, antitubercular, anti-inflammatory, anticancer, antiviral, antifungal, and antioxidant activities. The thiazolidinone nucleus is considered an important

pharmacophore capable of interacting effectively with biological targets through hydrogen bonding and hydrophobic interactions.

Pyridine-containing compounds are also well known for their significant therapeutic importance. Incorporation of pyridine moieties into heterocyclic frameworks often enhances biological activity, improves solubility, and increases binding affinity toward target proteins. Therefore, the combination of thiazolidinone and pyridine scaffolds may provide promising lead compounds for the development of effective antitubercular agents [8-14]. In recent years, computational approaches such as molecular docking and ADMET prediction studies have become valuable tools in modern drug discovery and development. Molecular docking helps predict ligand–protein interactions and binding affinity, while ADMET analysis provides important information regarding absorption, distribution, metabolism, excretion, and toxicity profiles of drug candidates. These computational approaches significantly reduce the time, cost, and failure rate associated with conventional drug discovery processes and assist in identifying promising lead molecules with favourable pharmacokinetic properties.

Based on these considerations, the present study was undertaken to synthesize a series of novel N-(4-oxo-3-aryl-1,2-thiazolidin-2-yl) pyridine-3-carboxamide derivatives and evaluate their antitubercular activity against *Mycobacterium tuberculosis* H37Rv strain. The synthesized compounds were characterized using FT-IR and ^{1}H NMR spectroscopy. Furthermore, in silico drug-likeness evaluation, bioactivity prediction, ADMET studies, and molecular docking analyses were performed to investigate their pharmacological potential and binding interactions with the target protein. The study aims to identify promising thiazolidinone derivatives that could serve as potential lead molecules for future antitubercular drug development.

Scheme

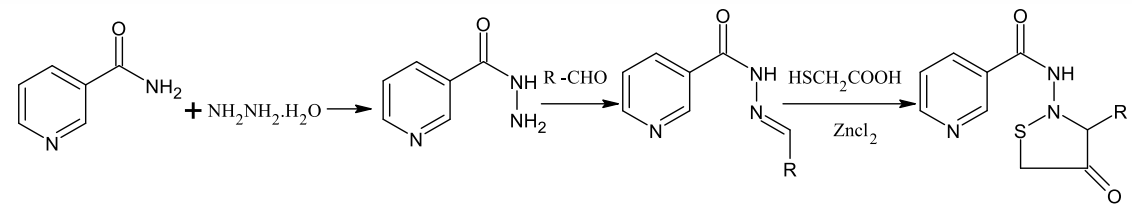

pyridine-3-carboxamide

pyridine-3-carbohydrazide **(1)**

N'-(arylmethylidene) pyridine-3-carbohydrazide **2 (a -e)**

N-(4-oxo-3-aryl-1,2-thiazolidin-2-yl) pyridine-3-carboxamide

R = **a**- 4-hydroxy phenyl,**b**-phenyl,**c**-2-furyl,**d**-2-chloro phenyl,**e**-4-methoxy phenyl

2. Physical Characterization

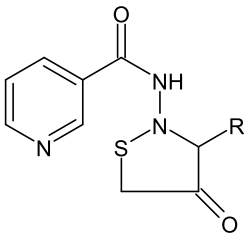

Table 1: Physical characterization of synthesized N-(4-oxo-3-aryl-1,2-thiazolidin-2-yl) pyridine-3-carboxamide derivatives 3(a-e):

S.No	Compounds (R	%Yield W/W	Melting point (°C)	Rf value	Molecular Formula	Molecular Weight	Composition%				
							C	H	N	O	S
3a	4-hydroxy Phenyl	72.68	173-175	0.78	$C_{15}H_{13}N_3O_3S$	315.34	57.13	4.16	13.33	15.22	10.17
3b	Phenyl	69.48	192-195	0.89	$C_{15}H_{13}N_3O_2S$	299.34	60.18	4.38	14.04	10.69	10.71
3c	2-furyl	65.43	183-185	0.73	$C_{13}H_{11}N_3O_2S$	289.30	53.97	3.83	14.52	16.59	11.08
3d	2-chloro phenyl	72.78	186-189	0.69	$C_{15}H_{12}ClN_3O_2S$	333.79	53.97	3.62	12.59 **Cl** 10.62	9.59	9.61
3e	4-methoxy Phenyl	79.80	159-162	0.63	$C_{16}H_{15}N_3O_3S$	329.37	58.34	4.59	12.76	14.57	9.74

Mobile phase - CHCl3:CH3OH: GAA ((90:10:01))

3. Spectral Characterization:

Table 2: IR & 1H NMR spectrum data of synthesized N-(4-oxo-3-aryl-1,2-thiazolidin-2-yl) pyridine-3-carboxamide derivatives 3(a-e):

S. No.	Compound (R)	IR Frequency (cm^{-1})	^1H NMR (δ, ppm)	Mass (m/z)
3a	4-Hydroxyphenyl	3648.90 (Ar–OH stretching), 3398.22 (N–H stretching), 3100.14 (Ar–C–H stretching), 1682.94 (C=O stretching), 1616.58 (C=C stretching), 1395.59 (Ar–C–N stretching), 1181.56 (C–S stretching)	4.03 (2H, d), 5.16 (1H, s), 6.69–7.57 (4H, m), 8.05–8.55 (3H, m), 8.91 (1H, s)	315
3b	Phenyl	3523.48 (N–H stretching), 3058.06 (Ar–C–H stretching), 1716.12 (C=O stretching), 1653.45 (C=O stretching), 1472.81 (Ar–C=C stretching), 1395.39 (Ar–C–N stretching), 1182.16 (C–S stretching)	4.77 (2H, d), 5.17 (1H, s), 7.28–7.63 (5H, m), 8.05–8.55 (3H, m), 8.91 (1H, s)	299
3c	2-Furyl	3488.48 (N–H stretching), 3023.48 (Ar–C–H stretching), 1701.38 (C=O stretching), 1616.58 (C=O stretching), 1421.19 (Ar–C=C stretching), 1303.22 (Ar–C–N stretching), 1244.23 (C–O–C stretching), 1177.88 (C–S stretching), 1030.41 (C–N stretching)	4.03 (2H, d), 5.05 (1H, s), 6.22–8.55 (7H, m), 8.91 (1H, s)	289
3d	2-Chlorophenyl	3481.62 (N–H stretching), 3059.90 (Ar–C–H stretching), 1749.08 (C=O stretching), 1653.45 (C=O stretching), 1421.19 (Ar–C=C stretching), 1188.94 (C–S stretching), 669.12 (C–Cl stretching)	4.03 (2H, d), 5.34 (1H, s), 7.07–7.34 (6H, m), 7.75–8.55 (3H, m), 8.91 (1H, s)	333
3e	4-Methoxyphenyl	3490.28 (N–H stretching), 3082.83 (Ar–C–H stretching), 1734.36 (C=O stretching), 1653.45 (C=O stretching), 1303.22 (Ar–C–N stretching), 1264.23 (C–O–C stretching), 1161.62 (C–S stretching)	3.75 (3H, s), 4.03 (2H, d), 5.23 (1H, s), 6.95–7.57 (6H, m), 8.05–8.55 (3H, m), 8.91 (1H, s)	329

4. Antitubercular Activity Evaluation

The antitubercular activity of the synthesized compounds was evaluated against *Mycobacterium tuberculosis* H37Rv using the Resazurin Microtiter Assay (REMA) plate method, a rapid and reliable technique for determining the minimum inhibitory concentration (MIC). The assay was performed to assess the inhibitory potential of the synthesized compounds against the growth of *M. tuberculosis* under *in vitro* conditions. Briefly, 100 µL of Middlebrook 7H9 broth medium containing the test microorganism was dispensed into each well of a sterile 96-well microtiter plate. The synthesized compounds were prepared at concentrations ranging from 1.25 to 10.0 µg/mL and added to the respective wells. To minimize evaporation during incubation, the peripheral wells of the plate were filled with sterile distilled water. A standardized bacterial suspension equivalent to McFarland standard No. 1 was prepared and further diluted (1:20) in 7H9 broth. Subsequently, 100 µL of the diluted inoculum was added to each test well. Wells containing inoculated medium without the test compound served as growth controls, while wells containing only sterile medium were maintained as negative controls. The plates were sealed and incubated at 37°C for seven days. Following incubation, 25 µL of freshly prepared 0.02% resazurin solution was added to each well, and the plates were incubated for an additional 48 hours. Resazurin acts as an oxidation–reduction indicator, changing from blue to pink in the presence of metabolically active bacterial cells. The MIC was defined as the lowest concentration of the test compound that prevented the color change from blue to pink, indicating complete inhibition of bacterial growth. The antitubercular susceptibility testing was carried out at AR Lab and Research Foundation, Salem, Tamil Nadu, India, following standard laboratory protocols for *M. tuberculosis* H37Rv evaluation. This method provided a quantitative assessment of the antimycobacterial potential of the synthesized compounds and facilitated comparison with established antitubercular agents.

Anti-tubercular activity of synthesized compounds (3a-3e) against *Mycobacterium tuberculosis* $H_{37}R_v$

Figure:1 Graphical representation of Anti tubercular activity of synthesized *N*-(4-oxo-3-aryl-1,2-thiazolidin-2-yl) pyridine-3-carboxamide derivatives 3(a-e)

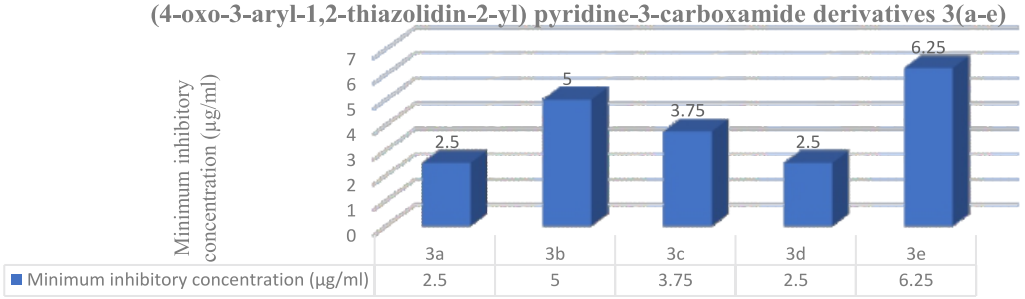

5. COMPUTATIONAL METHODOLOGY

5.1 Molinspiration Physicochemical and Bioactivity Prediction

The physicochemical properties and bioactivity scores of the synthesized compounds were evaluated using the Molinspiration Cheminformatics online server. Parameters, including molecular weight (MW), logarithm of partition coefficient (logP), topological polar surface area (TPSA), number of hydrogen bond donors and acceptors, number of rotatable bonds, and Lipinski's Rule of Five violations, were calculated to assess drug-likeness properties. Bioactivity scores for GPCR ligand, ion channel modulator, kinase inhibitor, nuclear receptor ligand, protease inhibitor, and enzyme inhibitor activities were also predicted using Molinspiration software.

5.2 ADMET Prediction Studies

The ADMET (Absorption, Distribution, Metabolism, Excretion, and Toxicity) properties of the synthesized compounds were predicted using the pkCSM online pharmacokinetic prediction server. The canonical SMILES of the synthesized compounds were used as input for the prediction of pharmacokinetic parameters, including water solubility, intestinal absorption, Caco-2 permeability, blood–brain barrier permeability, cytochrome P450 interactions, total clearance, AMES toxicity, hepatotoxicity, hERG inhibition, and skin sensitization.

The obtained results were analyzed to evaluate the drug-likeness and safety profiles of the synthesized compounds.

5.3 Molecular Docking Studies

Molecular docking studies were carried out using AutoDock Vina to evaluate the binding affinity and interaction of the synthesized compounds with the *Mycobacterium tuberculosis* enoyl-acyl carrier protein reductase (InhA) target protein. The three-dimensional crystal structure of the target protein was obtained from the Protein Data Bank (PDB).

Protein preparation involved the removal of water molecules and co-crystallized ligands, followed by the addition of polar hydrogen atoms and Kollman charges before docking analysis. Energy minimization of the protein structure was performed to obtain a stable conformation for docking studies. The ligand structures were drawn, optimized, and converted into appropriate PDBQT file formats using molecular modeling tools.

Grid box dimensions were defined around the active binding site of the InhA protein to ensure proper accommodation of ligands during docking simulations. Docking calculations were performed to predict the most favourable binding conformations based on minimum binding energy values. The docking interactions, hydrogen bonding, hydrophobic interactions, and binding poses of the synthesized compounds within the active site were analyzed using molecular visualization software.

Computational Techniques

Table 3: Molinspiration Physicochemical Evaluation for Drug-Likeness

C.No	Comp.	M/W	logP	TPSA	n atom	nON	nOHNH	nviolation	Nrotb	Volume	Acceptor	donors	Surface area
3a	4-hydroxyphenyl	315.35	0.53	82.53	22	6	2	0	3	263.38	6	2	130.818
3b	Phenyl	299.36	1.01	62.30	21	5	1	0	3	255.37	5	1	132.388
3c	2-furyl	289.32	0.27	75.44	20	6	1	0	3	236.93	6	1	118.818
3d	2-chloro phenyl	333.80	1.64	62.30	22	5	1	0	3	268.90	5	1	136.327
3e	4-methoxyphenyl	371.46	2.25	71.53	26	6	1	0	5	330.54	6	1	156.597

MW = molecular weight;
logP= logarithm of the partition coefficient between octanol and water;
TPSA = topological polar surface area;
n atom =number of atoms present in a given molecule (This value is often used to assess the potential for hydrogen bonding, acidity/basicity, and other functional group characteristics in the molecule);
nON = number of hydrogen bond acceptors (N and O atoms);
nOHNH = the number of hydroxyl (OH) and amine (NH) groups in a given molecule;
a_don = number of hydrogen bond donors;
a_acc = number of hydrogen bond acceptors;
Nrotb = number of rotatable bonds;
nViolation = number of Lipinski's Rule of Five violations (nViolation value of 0 would indicate no structural issues or violations, meaning the molecule follows standard bonding and stereochemical conventions)

Table 4: Molinspiration bioactivity score

C. No	Compound	GPCR ligand	Ion channel modulator	Kinase inhibitor	Nuclear receptor ligand	Protease inhibitor	Enzyme inhibitor
3a	4-hydroxyphenyl	-0.01	-0.16	-0.15	-0.21	0.01	0.09
3b	Phenyl	-0.11	-0.29	-0.25	-0.40	-0.07	-0.04
3c	2-furyl	-0.33	-0.51	-0.53	-0.61	-0.21	-0.16
3d	2-chloro phenyl	-0.08	-0.26	-0.34	-0.36	-0.12	-0.06
3e	4-methoxy phenyl	-0.05	-0.14	-0.20	-0.12	0.16	0.12

Table 5: Standard value for ADMET

PROPERTIES	MODEL NAME	STANDARD VALUE	
Absorption	Water solubility (log mol/L)	0.001-0.1 mol/L	Slightly soluble
		<0.001 mol/L	Insoluble
Absorption	Caco2 Permeability (log P_{app} in 10^{-6} cm/s)	<0.90	Low Permeability
		0.90–1.50	Moderate permeability
		>1.50	High Permeability
Absorption	Intestinal Absorption (%)	80-90%	Absorption for most nutrients
Absorption	Skin permeability (log Kp)	-8 to-1	Better skin permeability
		Nearly -8	Very low skin permeability
Absorption	P-glycoprotein substrate	Efflux ratio at least 2	The drug is actively pumped out of the cell
Absorption	P-glycoprotein I inhibitor	IC 50(half maximal inhibitory concentration) within the range of 1-10 µM	Potent inhibitors
Absorption	P-glycoprotein II inhibitor	IC 50 value in the low µM range	Potent inhibitors
Distribution	VDss (human) (log L/kg)	< 0.6	Low VDss
		0.6-5	Medium VDss
		> 5	High VDss
Distribution	Fraction Unbound (Human) (Fu)	Greater than 0.5 or 50%	Low protein binding in the blood
		Less than 0.1 or 10%	High protein binding in the blood
Distribution	BBB permeability (log BB)	>0.3	High BBB permeability
		<-1	Poor BBB permeability
		Between 0.3 and -1	Moderate BBB permeability
Distribution	CNS permeability (log PS)	>-2	Better CNS permeability
		Below -2	Poor CNS permeability
Metabolism	CYP2D6 Substrate	NO	
Metabolism	CYP3A4 Substrate	YES	

Metabolism	CYP1A2 Inhibitor	YES	
Metabolism	CYP2C19 Inhibitor	YES	
Metabolism	CYP2C9 Inhibitor	NO	
Metabolism	CYP2D6 Inhibitor	NO	
Metabolism	CYP3A4 Inhibitor	NO	
Excretion	Total Clearance (log ml/min/kg)	Male	97 to 137 mL/min (1.65 to 2.33 mL/s)
		Female	88 to 128 mL/min (1.467 to 2.18)
Excretion	Renal OCT2 substrate	Renal organic cation transporter 2 (OCT2)	1860 µmol/L
Toxicity	AMES toxicity	NO	
Toxicity	Max. tolerated dose (human) (log mg/kg/day)	Low or Non-toxic	≤ 0.477
		High or Toxic	>0.477
Toxicity	hERG I inhibitor	NO	
Toxicity	hERG II inhibitor	NO	
Toxicity	Oral Rat Acute Toxicity (LD50) (mol/kg)	Non-toxic	2.5947
Toxicity	Oral Rat Chronic Toxicity (LOAEL) (log mg/kg-bw/day)	Lowest observed adverse effect level	0.005-0.040 g/kg-bw/day)
Toxicity	Hepatotoxicity	Grade 1 (mild)	Between 1.25 and <2.5
		Grade 2 (Moderate)	Between 2.5 and <5.0
		Grade 3 (serious)	Between 5.0 and <10
		Grade 4 (Acute liver failure)	≥ 10
		Grade 5 (death)	Liver transplantation
Toxicity	Skin sensitization	Low EC_3 Value	Strong skin sensitization
		High EC_3 Value	Weaker skin sensitization
Toxicity	T.Pyriformis toxicity (log µg/L)	Non-toxic	0
		Toxic	1

Table 6: ADMET Predictions for Absorption

C.No	Compound	Absorption						
		Water solubility (log mol/L)	$Caco_2$ Permeability (log P_{app} in 10^{-6} cm/s)	Intestinal Absorption %	Skin permeability (log Kp)	P-glycoprotein substrate (Categorical value)	P-glycoprotein 1 inhibitor (Categorical value)	P-glycoprotein II inhibitor (Categorical value)
3a	4-hydroxyphenyl	-3.208	1.071	94.397	-3.111	No	No	No
3b	phenyl	-3.807	1.373	95.295	-3.064	Yes	No	No
3c	2-furyl	-3.317	0.785	94.572	-3.448	No	No	No
3d	2-chlorophenyl	-4.064	0.944	93.704	-3.228	No	No	No
3e	4-methoxy phenyl	-4.79	1.44	94.712	-3.001	No	Yes	Yes

Table 7: ADMET Predictions for Distribution

C.No	Compound	Distribution			
		VDss (human) (log L/kg)	Fraction Unbound (Human)(Fu)	BBB permeability (log BB)	CNS permeability (log PS)
3a	4-hydroxy phenyl	-0.232	0.248	-0.487	-2.961
3b	phenyl	-0.292	0.121	-0.127	-2.872
3c	2-furyl	-0.423	0.463	-0.681	-3.089
3d	2-chloro phenyl	-0.295	0.131	-0.057	-2.269
3e	4-methoxyphenyl	-0.312	0.321	-0.612	-2.347

Table 8: ADMET Predictions for Excretion

C.No	Compound	Excretion	
		Total Clearance	Renal OCT2 substrate
3a	4-hydroxy phenyl	-0.125	No
3b	phenyl	-0.065	No
3c	2-furyl	0.162	No
3d	2-chloro phenyl	-0.075	No
3e	4-methoxyphenyl	-0.284	No

Table 9: ADMET Predictions for Metabolism

C.No	Compound	Metabolism						
		CYP2D6 Substrate (Yes/No)	CYP3A4 Substrate (Yes/No)	CYP1A2 Inhibitor (Yes/No)	CYP2C19 Inhibitor (Yes/No)	CYP2C9 Inhibitor (Yes/No)	CYP2D6 Inhibitor (Yes/No)	CYP3A4 Inhibitor (Yes/No)
3a	4-hydroxy phenyl	No	No	Yes	No	No	No	No
3b	phenyl	No	Yes	Yes	Yes	No	No	No
3c	2-furyl	No	No	No	No	No	No	No
3d	2-chloro phenyl	No	Yes	Yes	Yes	No	No	No
3e	4-methoxyphenyl	No	Yes	No	Yes	Yes	No	No

Table 10: ADMET Predictions for Toxicity

C.NO	Compound	Toxicity									
		AMES toxicity (Yes/No)	Max.tolerateddose(human) (log mg/kg/day)	hERG I inhibitor	hERG II inhibitor	Oral Rat Acute Toxicity (LD50) (mol/kg)	Oral Rat Chronic Toxicity (LOAEL) (log mg/kg-bw/day)	Hepatotoxicity (Yes/No)	Skin sensitization (Yes/No)	T.Pyriformis toxicity (log µg/L)	Minnow toxicity (log mM)
3a	4-hydroxy phenyl	No	0.048	No	No	2.443	1.474	No	No	0.664	0.419
3b	Phenyl	No	0.08	No	No	2.618	1.155	No	No	0.82	0.801
3c	2-furyl	No	0.117	No	No	2.513	1.204	Yes	No	0.322	2.257
3d	2-chloro phenyl	No	0.288	No	No	2.754	1.359	Yes	No	1.023	-0.44
3e	4-methoxy phenyl	No	0.122	No	No	2.848	1.834	Yes	Yes	0.834	-0.008

compounds 3c, 3d, and 3e were predicted to exhibit hepatotoxic potential.

Table 11: Docking scores

C. No	Compound	CurPocket ID	Vina Score	Cavity Volume (Å³)	Center (x,y,z)	Docking Size (x,y,z)
3a	4-hydroxy phenyl	C1	-8.6	1108	-32, -9, -16	22,22,22
		C2	-8.5	1053	-52,3,8	22,22,22
		C3	-8.4	917	-26,29, -11	22,22,22
		C4	-7.9	645	-14,10,13	22,22,22
		C5	-5.7	617	-28,10, -19	22,22,22
3b	Phenyl	C1	-8.6	1108	-32, -9, -16	21,21,21
		C2	-8.5	1053	-52,3,8	21,21,21
		C3	-8.3	917	-26,29, -11	21,21,21
		C4	-8.3	645	-14,10,13	21,21,21
		C5	-6.2	617	-28,10, -19	21,21,21
3c	2-furyl	C1	-7.8	1108	-32, -9, -16	21,21,21
		C2	-7.5	1053	-52,3,8	21,21,21
		C3	-7.7	917	-26,29, -11	21,21,21
		C4	-7.5	645	-14,10,13	21,21,21
		C5	-5.8	617	-28,10, -19	21,21,21
3d	2-chloro phenyl	C1	-7.8	1108	-32, -9, -16	21,21,21
		C2	-7.9	1053	-52,3,8	21,21,21
		C3	-7.9	917	-26,29, -11	21,21,21
		C4	-7.9	645	-14,10,13	21,21,21
		C5	-5.7	617	-28,10, -19	21,21,21
3e	4-methoxyphenyl	C1	-8.3	1108	-32, -9, -16	21,21,21
		C2	-7.9	1053	-52,3,8	21,21,21
		C3	-7.5	917	-26,29, -11	21,21,21
		C4	-7.6	645	-14,10,13	21,21,21
		C5	-7.5	617	-28,10, -19	21,21,21

Molecular Docking Figures

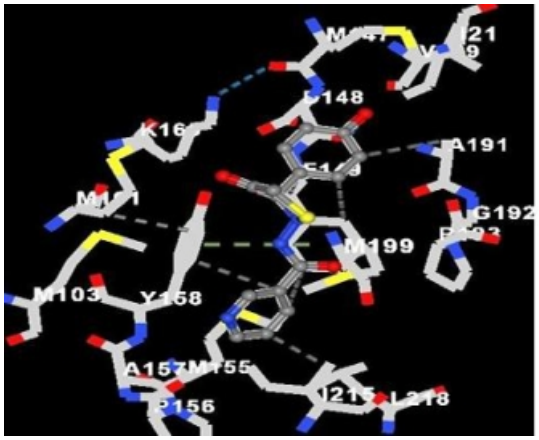

FIGURE I: N-(4-oxo-3-aryl-1,2-thiazolidin-2-(p-hyroxy phenyl) pyridine-3-carboxamide(3a)

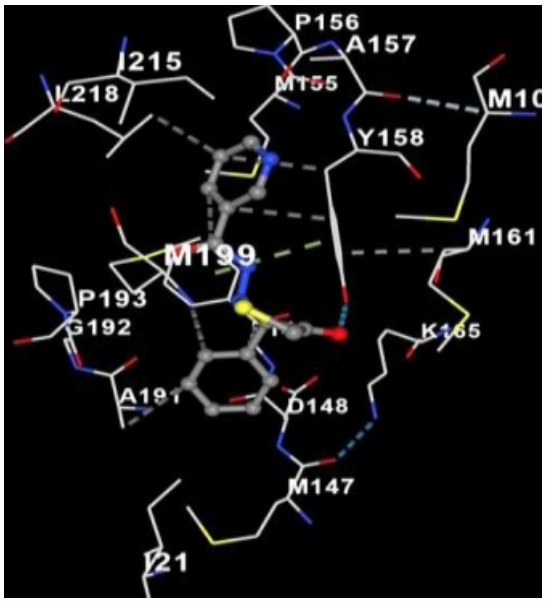

FIGURE 2: N-(4-oxo-3-aryl-1,2-thiazolidin-2-(phenyl) pyridine-3-carboxamide (3b)

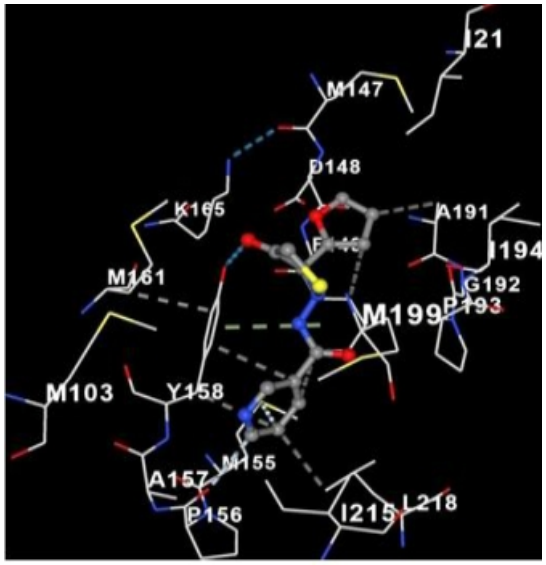

FIGURE 3: N-(4-oxo-3-aryl-1,2-thiazolidin-2-(2-furyl) pyridine-3-carboxamide(3c)

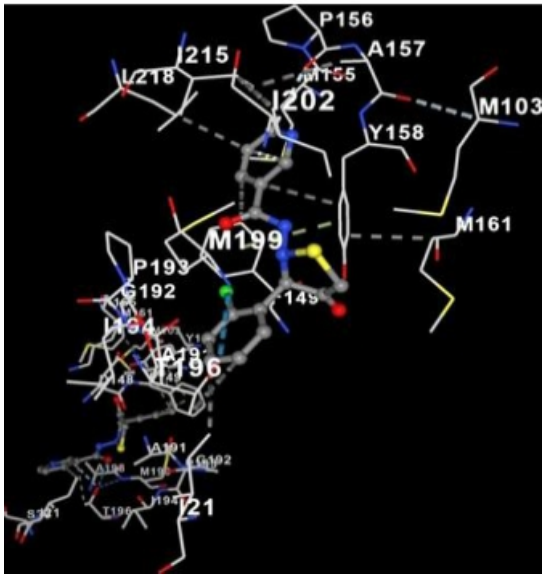

FIGURE 4: N-(4-oxo-3-aryl-1,2-thiazolidin-2-(m-chloro phenyl) pyridine-3-carboxamide(3d)

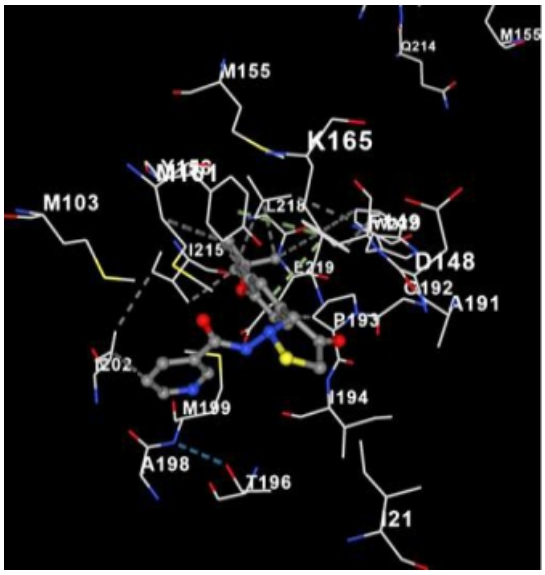

FIGURE 5: N-(4-oxo-3-aryl-1,2-thiazolidin-2-(p-methroxy phenyl) pyridine-3-carboxamide(3e)

5. RESULTS AND DISCUSSION

5.1 Spectral Characterization

FT-IR Spectroscopy

The synthesized N-(4-oxo-3-aryl-1,2-thiazolidin-2-yl) pyridine-3-carboxamide derivatives 3(a–e) were characterized by FT-IR spectroscopy, and the obtained spectral data confirmed the successful formation of the target compounds. Characteristic absorption bands corresponding to important functional groups were observed in all synthesized derivatives.

Broad absorption bands observed in the region 3481.62–3648.90 cm^{-1} confirmed the presence of hydroxyl (–OH) and amide (>N–H) stretching vibrations. Aromatic C–H stretching vibrations appeared in the range of 3023.48–3100.14 cm^{-1}, indicating the presence of aromatic moieties in all compounds. Strong absorption bands observed between 1682.94–1749.08 cm^{-1} corresponded to carbonyl (C=O) stretching vibrations of the thiazolidinone and amide functionalities.

The aromatic C=C stretching vibrations were observed around 1421.19–1472.81 cm^{-1}, while aromatic C–N stretching vibrations appeared in the range of 1303.22–1395.59 cm^{-1}. Characteristic C–S stretching vibrations of the thiazolidinone ring were observed at 1161.62–1188.94 cm^{-1}, confirming cyclization and formation of the thiazolidinone nucleus. In compound 3d, the presence of a C–Cl stretching vibration at 669.12 cm^{-1} further confirmed substitution of the chlorophenyl group. Similarly, compounds containing methoxy and furyl substituents exhibited characteristic C–O–C stretching vibrations in the range of 1244.23–1264.23 cm^{-1}.

Overall, the FT-IR spectral data strongly supported the successful synthesis of the designed thiazolidinone derivatives.

^{1}H NMR Spectroscopy

The ^{1}H NMR spectral analysis further confirmed the structures of the synthesized compounds 3(a–e).

The spectra showed characteristic signals corresponding to the thiazolidinone ring, aromatic protons, and substituted functional groups.

The methylene protons (CH_2) of the thiazolidinone ring appeared as doublets around δ 4.03–4.77 ppm, confirming formation of the heterocyclic ring system. The methine proton attached to the thiazolidinone ring appeared as a singlet at δ 5.05–5.34 ppm. Aromatic protons were observed as multiplets in the range of δ 6.22–8.55 ppm, corresponding to substituted phenyl, furyl, and pyridine ring protons.

The amide NH proton appeared as a singlet around δ 8.91 ppm in all compounds, indicating the presence of the carboxamide linkage. In compound 3e, methoxy group protons appeared as a singlet at δ 3.75 ppm, confirming the presence of the methoxy substituent. Compound 3a exhibited characteristic signals attributable to the hydroxyl-substituted aromatic ring.

Thus, the obtained ^{1}H NMR spectral data were in good agreement with the proposed structures of the synthesized thiazolidinone derivatives.

5.2 Antitubercular Activity

The synthesized compounds 3(a–e) were evaluated for antitubercular activity against *Mycobacterium tuberculosis* H37Rv strain using the Resazurin Microtiter Assay (REMA) plate method. The minimum inhibitory concentration (MIC) values indicated that all synthesized compounds exhibited appreciable antitubercular activity against the tested organism.

Among the synthesized derivatives, compounds 3a and 3d demonstrated significant antitubercular activity, suggesting that hydroxy and chloro substituents on the aromatic ring enhance biological activity. Compound 3b exhibited comparatively better activity among the tested derivatives, while compound 3c showed moderate inhibitory activity against *Mycobacterium tuberculosis*. Compound 3e displayed moderate activity, possibly due to the electron-donating methoxy substituent influencing interaction with the biological target.

The observed activity may be attributed to the presence of the thiazolidinone nucleus combined with the pyridine carboxamide moiety, which are known pharmacophores for antimycobacterial activity. Variations in aromatic substituents significantly influenced the biological activity of the synthesized compounds.

5.3 Physicochemical Evaluation for Drug-Likeness

The physicochemical properties of compounds 3(a–e) were evaluated using Molinspiration software, and the calculated parameters indicated favourable drug-like characteristics for the synthesized compounds.

The molecular weights of the synthesized compounds ranged from 289.30 to 333.79 g/mol, which fall within the acceptable range suggested by Lipinski's Rule of Five, indicating good oral drug-likeness. The calculated logP values ranged from 0.27 to 2.25, demonstrating moderate lipophilicity and suggesting favourable membrane permeability and absorption characteristics.

The TPSA values for all synthesized compounds were found within the acceptable range of 62.30–82.53 Å^2, suggesting good oral bioavailability and adequate hydrogen bonding capacity. All compounds possessed acceptable numbers of hydrogen bond donors and acceptors and exhibited zero Lipinski violations, indicating compliance with standard drug-likeness criteria.

The number of rotatable bonds ranged from 3 to 5, suggesting moderate molecular flexibility, which may facilitate better fitting within biological target active sites while maintaining structural stability.

Overall, the physicochemical evaluation demonstrated that the synthesized compounds possess favourable drug-like properties and may serve as potential candidates for further biological investigation.

5.4 Molinspiration Bioactivity Score Analysis

The Molinspiration bioactivity score analysis was performed to predict possible biological interactions of the synthesized compounds with various pharmacological targets, including GPCR ligands, ion channel modulators, kinase inhibitors, nuclear receptor ligands, protease inhibitors, and enzyme inhibitors.

Among the synthesized derivatives, compound 3e exhibited comparatively better bioactivity scores, particularly as a protease inhibitor and enzyme inhibitor, suggesting potential interaction with enzymatic targets. Compound 3a also showed moderate activity as an enzyme inhibitor and a protease inhibitor.

Compounds 3b and 3d displayed moderate negative scores across most categories, indicating comparatively lower biological interactions. Compound 3c showed the least favourable bioactivity scores among the synthesized derivatives, suggesting weaker interactions with the studied biological targets.

The bioactivity results indicate that electron-donating substituents such as methoxy and hydroxy groups may enhance biological interactions, whereas heterocyclic substitutions such as furyl rings may reduce predicted activity.

5.5 ADMET Prediction Studies

The ADMET properties of compounds 3(a–e) were predicted using pkCSM software to evaluate their pharmacokinetic and toxicity profiles.

Absorption Properties

All synthesized compounds demonstrated high predicted intestinal absorption values (>93%), indicating favourable oral bioavailability. Compounds 3b and 3e exhibited relatively higher Caco-2 permeability values, suggesting enhanced membrane permeability and absorption potential.

Water solubility analysis indicated that compounds 3a and 3c possessed comparatively better aqueous solubility, while compounds 3d and 3e were less soluble due to increased lipophilicity.

Most compounds were predicted to be non-substrates of P-glycoprotein, except compounds 3b and 3e, which may undergo efflux-mediated transport.

Distribution Properties

The predicted VDss values suggested low tissue distribution for all compounds. The BBB permeability values indicated poor penetration across the blood–brain barrier, suggesting limited central nervous system exposure. Similarly, the CNS permeability values also confirmed poor CNS distribution.

Metabolism

The metabolic predictions revealed that compounds 3b, 3d, and 3e are substrates for CYP3A4 enzymes, indicating possible hepatic metabolism through cytochrome-mediated pathways. Compounds 3b and 3d were predicted to inhibit CYP1A2 and CYP2C19 enzymes, while compound 3e additionally inhibited CYP2C9.

Excretion

The total clearance values suggested slow elimination of the compounds from the body, which may contribute to prolonged biological activity. None of the synthesized derivatives was predicted to be substrates of renal OCT2 transporters.

Toxicity Studies

The toxicity predictions demonstrated that all synthesized compounds were non-mutagenic according to the AMES toxicity test. None of the compounds was predicted to inhibit hERG channels, indicating low cardiotoxic potential.

Compounds 3c, 3d, and 3e showed mild hepatotoxicity predictions, whereas compounds 3a and 3b were predicted to be non-hepatotoxic. Compound 3e exhibited possible skin sensitization, while other compounds were predicted to be non-sensitizers.

Overall, the ADMET analysis suggested that the synthesized compounds possess acceptable pharmacokinetic profiles with relatively low toxicity risks.

5.6 Molecular Docking Studies

Molecular docking studies were performed using AutoDock Vina to evaluate binding interactions between the synthesized compounds and the selected *Mycobacterium tuberculosis* enoyl-acyl carrier protein reductase (InhA) target protein. Before docking, the target protein structure was prepared by removing water molecules and co-crystallized ligands, followed by the addition of polar hydrogen atoms and Kollman charges. The prepared protein and ligand structures were converted into PDBQT format for docking analysis.

The docking scores indicated favourable binding affinities toward the protein active site. Among the synthesized compounds, 3a and 3b demonstrated the best docking scores (–8.6 kcal/mol) within cavity C1, indicating strong interactions with the active site of the target protein. Compound 3e also exhibited good binding affinity with a docking score of –8.3 kcal/mol.

The cavity volumes ranged from 617 to 1108 Å^3, suggesting adequate space for ligand accommodation within the binding pockets.

The docking dimensions and cavity centers confirmed stable fitting of the synthesized compounds within the receptor active sites.

The enhanced binding affinity observed for compounds containing hydroxy and phenyl substituents may be attributed to hydrogen bonding interactions and hydrophobic contacts with amino acid residues present in the active site. The docking studies supported the experimental antitubercular activity results and indicated that the synthesized thiazolidinone derivatives may act as promising antitubercular agents.

5.7 Structure–Activity Relationship (SAR)

Electron-withdrawing substituents such as chloro groups enhanced activity, possibly due to increased hydrophobic interactions within the target binding pocket. Hydroxy substitution may improve activity through hydrogen bonding interactions with active-site residues, thereby enhancing ligand binding affinity.

Compounds containing unsubstituted phenyl rings also demonstrated good activity, suggesting that aromatic hydrophobic interactions contribute positively to receptor binding. In contrast, the methoxy-substituted derivative exhibited comparatively moderate activity, indicating that strong electron-donating groups may reduce optimal ligand–target interactions.

The furyl-substituted derivative displayed moderate biological activity, which may be attributed to altered electronic distribution and weaker hydrophobic interactions compared with phenyl-substituted analogues.

Overall, the SAR findings suggest that both electronic and hydrophobic properties of aromatic substituents play crucial roles in determining the antitubercular activity of thiazolidinone derivatives.

CONCLUSION

The present study successfully synthesized a series of novel N-(4-oxo-3-aryl-1,2-thiazolidin-2-yl) pyridine-3-carboxamide derivatives and characterized them using FT-IR and ^{1}H NMR spectral analyses. The spectral data confirmed the successful formation of the desired thiazolidinone framework.

Biological evaluation revealed promising antitubercular activity for all synthesized compounds against *Mycobacterium tuberculosis* H37Rv strain. Compounds containing hydroxy and chloro substituents demonstrated comparatively better activity, indicating the significant influence of substituent effects on biological performance.

The in-silico drug-likeness, ADMET, and molecular docking studies further supported the potential of these compounds as promising antitubercular candidates. Most compounds exhibited favourable pharmacokinetic properties, acceptable toxicity profiles, and strong binding affinities toward the *Mycobacterium tuberculosis* enoyl-acyl carrier protein reductase (InhA) target protein. Among the synthesized derivatives, compounds 3a, 3b, and 3d emerged as the most promising candidates for further optimization and biological investigation as potential antitubercular agents.

Overall, the combined experimental and computational findings suggest that these thiazolidinone derivatives may serve as promising lead compounds for the development of novel antitubercular drugs. Further structural optimization, detailed mechanistic studies, and *in vivo* investigations are warranted to establish their therapeutic potential and safety profiles.

References

1. Bontha Venkata Subramanya Lokesh et al., (2019). "Synthesis, Biological Evaluation and Molecular Docking Studies of New Pyrazolines as Anti-Tubercular and Cytotoxic Agents." *Bioorganic Chemistry*, pp. 1–12.
2. Katharigatta N. Venugopala et al., (2021). "Molecular Docking and Anti-Tubercular Evaluation of Designed Compounds." *Journal of Molecular Structure*, pp. 129245–129256.
3. N. C. Desai et al., (2016). "Synthesis, Biological Evaluation and Molecular Docking Study of Novel Indole and Pyridine Based 1,3,4-Oxadiazole Derivatives as Potential Anti-Tubercular Agents." *Bioorganic & Medicinal Chemistry Letters*, pp. 1776–1783.
4. Sarvesh Kumar Pandey et al., (2020). "Synthesis, Biological Evaluation and Molecular Docking Studies of Novel Quinazolinones as Anti-Tubercular and Anti-Malarial Agents." *European Journal of Medicinal Chemistry*, pp. 112867–112879.
5. Mayursinh Zala et al., (2023). "Synthesis, Characterization, Anti-Tubercular Activity and Molecular Docking Studies of Pyrazolylpyrazoline-Clubbed Triazole and Tetrazole Hybrids." *Journal of Molecular Structure*, pp. 135430–135438.
6. Mubarak H. Shaikh et al., (2015). "1,2,3-Triazole Derivatives as Anti-Tubercular Agents: Synthesis, Biological Evaluation and Molecular Docking Study." *Medicinal Chemistry Research*, pp. 149–158.
7. Esra Tatar et al., (2016). "Design, Synthesis and Molecular Docking Studies of a Conjugated Thiadiazole-Thiourea Scaffold as Anti-Tubercular Agents." *Bioorganic Chemistry*, pp. 1–9.
8. Shankar Thapa et al., (2024). "Synthesis, Molecular Docking, Molecular Dynamic Simulation Studies and Anti-Tubercular Activity Evaluation of Substituted Benzimidazole Derivatives." *Journal of Biomolecular Structure and Dynamics*, pp. 1–15.
9. Pimonluck Sittikornpaiboon et al., (2016). "Molecular Docking Study of *Mycobacterium tuberculosis* Dihydrofolate Reductase in Complex with 2,4-Diaminopyrimidine Analogues." *Journal of Molecular Graphics and Modelling*, pp. 223–230.
10. Pran Kishore Deb et al., (2021). "In Vitro Anti-TB Properties, In Silico Target Validation, Molecular Docking and Dynamics Studies of Substituted 1,2,4-Oxadiazole Analogues against *Mycobacterium tuberculosis*." *Computers in Biology and Medicine*, pp. 104984–104995.
11. Nilam H. Lalavani et al., (2022). "Synthesis, Pharmacokinetic and Molecular Docking Studies of New Benzohydrazide Derivatives Possessing Anti-Tuberculosis Activity." *Journal of Molecular Structure*, pp. 132569–132577.
12. M. J. Zala et al., (2022). "Synthesis and Molecular Docking Study of Arylsulfanyl Pyrazolylpyrazoline Derivatives as Anti-Tubercular Agents." *Synthetic Communications*, pp. 2438–2450.

13. S. Bodige et al., (2020). "Design, Synthesis, Anti-Tubercular and Antibacterial Activities of 1,3,5-Triazinyl Carboxamide Derivatives and In Silico Docking Studies." *Chemical Biology & Drug Design*, pp. 601–612.
14. B. Srinu et al., (2019). "Synthesis, Anti-Tubercular Activity and Molecular Docking Studies of Novel Pyrimidine-5-Carboxamides." *Medicinal Chemistry Research*, pp. 1200–1210.
15. H. Surya Prakash Rao et al., (2023). "Design, Synthesis, Molecular Docking and Biological Activity of Pyrazolo[3,4-b] Pyridines against *M. tuberculosis*." *Journal of Heterocyclic Chemistry*, pp. 1450–1462.
16. Sravanthi Siliveri et al., (2024). "Design, Synthesis, In Silico Molecular Docking, ADMET Studies and Biological Evaluation of Novel Diphenyl Pyrazole Incorporated Triazolyl Benzene Sulfonamides." *Results in Chemistry*, pp. 101234–101245.
17. Sushil K. Kashaw et al. (2011). "Synthesis and Anti-Tubercular Evaluation of Novel Thiazolidinones and Brominated Derivatives." *European Journal of Medicinal Chemistry*, pp. 384–390.
18. Nazar Trotsko et al., (2021). "Anti-Tubercular Properties of Thiazolidin-4-ones." *Bioorganic Chemistry*, pp. 105321–105335.
19. Himaja Malipeddi et al., (2012). "Synthesis and Anti-Tubercular Activity of Novel Thiazolidinone Derivatives." *International Journal of Pharmaceutical Sciences and Research*, pp. 221–227.
20. Haresh Oza et al., (1998). "Synthesis and Anti-Tubercular Activity of Thiazolidinone Derivatives." *Indian Journal of Chemistry*, pp. 1045–1049.